

Correlated Chern insulators in two-dimensional Raman lattices: a cold-atom regularization of strongly-coupled four-Fermi field theories

L. Ziegler,¹ E. Tirrito,^{2,3} M. Lewenstein,^{3,4} S. Hands,⁵ and A. Bermudez¹

¹*Departamento de Física Teórica, Universidad Complutense, 28040 Madrid, Spain*

²*International School for Advanced Studies (SISSA), via Bonomea 265, 34136 Trieste, Italy*

³*ICFO - Institut de Ciències Fotoniques, The Barcelona Institute of Science and Technology,
Av. Carl Friedrich Gauss 3, 08860 Castelldefels (Barcelona), Spain*

⁴*ICREA, Lluís Companys 23, 08010 Barcelona, Spain*

⁵*Department of Physics, Faculty of Science and Engineering,
Swansea University, Singleton Park, Swansea SA28PP, United Kingdom*

We show that ultra-cold atoms with synthetic spin-orbit coupling in Raman lattices can be used as versatile quantum simulators to explore the connections between correlated Chern insulators and strongly-coupled four-Fermi field theories related to the Gross-Neveu model in (2+1) dimensions. Exploiting this multidisciplinary perspective, we identify a large- N quantum anomalous Hall (QAH) effect in absence of any external magnetic field, and use it to delimit regions in parameter space where these correlated topological phases appear, the boundaries of which are controlled by strongly-coupled fixed points of the four-Fermi relativistic field theory. We further show how, for strong interactions, the QAH effect gives way to magnetic phases described by a two-dimensional quantum compass model in a transverse field. We present a detailed description of the phase diagram using the large- N effective potential, and variational techniques such as projected entangled pairs.

The interplay of quantum mechanics and special relativity leads to the coupling of the intrinsic angular momentum of the electron with its own motion, underlying the fine structure of atomic spectra [1]. This so-called *spin-orbit coupling* (SOC) can be accounted for by the Dirac equation [2, 3] and, ultimately, by quantum electrodynamics [4]. Indeed, it is the comparison of perturbative calculations of this weakly-coupled quantum field theory (QFT) [5, 6] with high-precision measurements of the intrinsic magnetic moment of the electron [7] and the fine structure constant [8], which yields the most accurate tests of this QFT.

SOC has also become a cornerstone of modern condensed matter [9, 10], as it underlies the experimental discovery [11, 12] of a mechanism for the ordering of matter [13–15] characterised by the unique role of topology [16–18]. This is epitomised by Chern insulators [19–21], which have an insulating bulk with a non-zero topological invariant and, simultaneously, host current-carrying states at the boundaries. It is remarkable that elaborate concepts of algebraic topology [22], such as the first Chern number of a fibre bundle [23], emerge naturally from the band structure of these materials and, more importantly, that they become responsible for the robust quantisation of the transverse conductivity even without any external magnetic field, i.e. a quantum anomalous Hall effect [24, 25]. Besides their fundamental interest, topological materials can be used to build devices with novel functionalities and promising technological applications [26].

These SOC phenomena might seem rather simple at first sight, as topological insulators employ band-structure methods based on free electrons, whereas calculations for this QFT rely on perturbation theory about a weakly-coupled fixed point. Nonetheless, this simplicity is deceiving, as numerous open questions arise as one departs from these limits, exploring (i) topological phases in the presence of strong SOC and inter-particle interactions that can lead, for instance, to *correlated Chern insulators* and phase transitions thereof, or (ii) relativistic QFTs with SOC that are controlled by strongly-

coupled fixed points, the properties of which can only be accessed non-perturbatively. As argued here, these seemingly unrelated topics can be connected by considering SOC in light of specific discretizations [27] of *strongly-coupled four-Fermi QFTs* [28–30]. Originally introduced by Enrico Fermi in the context of the weak nuclear interactions [31], four-Fermi QFTs such as the Nambu-Jona-Lasinio [32] or Gross-Neveu [33] models are nowadays considered as effective QFTs that capture the essence of dynamical chiral symmetry breaking, a phenomenon relevant to the strong nuclear interactions. We show that, dispensing with the notion of chirality in the context of a 2D Hubbard model [34] with strong SOC, analogous strongly-coupled four-Fermi QFTs emerge in the long-wavelength limit of correlated Chern insulators.

This connection can be leveraged to develop non-perturbative studies of Chern insulators with interacting electrons following two strategies. On the one hand, one can interpret the lattice as a mere regularisation [35], and exploit the machinery of lattice field theories [36] to explore correlation effects, understanding the nature of the interaction-driven quantum phase transitions by connecting them to strongly-coupled fixed points. On the other hand, the connection to SOC suggests a different type of regularization. Rather than using the lattice as an artificial scaffolding for numerical computations, one may consider experimental setups, where this lattice is indeed physical, and both the SOC and four-Fermi interactions appear naturally. As discussed below, Fermi gases with synthetic SOC in optical lattices are a particularly-promising platform [37, 38], as they can provide a cold-atom regularisation of strongly-coupled QFTs and serve as quantum simulators [39–41] of correlated Chern insulators. Considering the shortage of topological materials where correlations have been shown to play a role, we believe that our results are encouraging, identifying cold atoms as a viable platform to explore the intricate connections of interacting topological matter and strongly-coupled relativistic QFTs.

The model.— We consider a Wilsonian discretization [27]

of a Hamiltonian QFT for N flavours of self-interacting Dirac

fields $\{\psi_c(\mathbf{x})\}_{c=1}^N$ which, in natural units, reads

$$H = a_1 a_2 \sum_{\mathbf{x} \in \Lambda_s} \left[\sum_{j=1,2} \left(-\bar{\Psi}(\mathbf{x}) \left(\frac{i\gamma^j}{2a_j} + \frac{r_j}{2a_j} \right) \Psi(\mathbf{x} + a_j \mathbf{e}_j) + \bar{\Psi}(\mathbf{x}) \left(\frac{m}{4} + \frac{r_j}{2a_j} \right) \Psi(\mathbf{x}) + \text{H.c.} \right) - \frac{g^2}{2N} \left(\bar{\Psi}(\mathbf{x}) \Psi(\mathbf{x}) \right)^2 \right], \quad (1)$$

where we introduced $\Psi(\mathbf{x}) = (\psi_1(\mathbf{x}), \dots, \psi_N(\mathbf{x}))^t$, $\bar{\Psi}(\mathbf{x}) = (\psi_1^\dagger(\mathbf{x})\gamma^0, \dots, \psi_N^\dagger(\mathbf{x})\gamma^0)$ is the adjoint, and $\gamma^0, \gamma^1, \gamma^2$ are the so-called gamma matrices for a (2+1)-dimensional space-time $\{\gamma^\mu, \gamma^\nu\} = 2g^{\mu\nu}\mathbb{I}$, where $g^{\mu\nu} = \text{diag}(1, -1, -1)$ is Minkowski's metric with spacetime indexes $\mu, \nu \in \{0, 1, 2\}$.

Inspired by the approach of Hamiltonian lattice field theories [42], in which only the spatial coordinates are discretised, we consider an anisotropic rectangular lattice $\Lambda_s = \{\mathbf{x} = n_1 a_1 \mathbf{e}_1 + n_2 a_2 \mathbf{e}_2, \forall (n_1, n_2) \in \mathbb{Z}_{N_1} \times \mathbb{Z}_{N_2}\}$ with lattice spacings a_1, a_2 along the Cartesian unit vectors $\mathbf{e}_1, \mathbf{e}_2$. In Eq. (1), we have also introduced the Wilson parameters $\{r_j\}$, a bare mass m , and a coupling g^2 that controls the strength of the simplest fermion-fermion interaction with Lorentz invariance. In the long-wavelength limit, one obtains 4 fermion doublers [43, 44], each described by a continuum QFT for an N -flavour Dirac spinor $\{\Psi_{\mathbf{n}_d}(\mathbf{x})\}_{\mathbf{n}_d}$, $\mathbf{n}_d = (n_{d,1}, n_{d,2}) \in \{0, 1\} \times \{0, 1\}$ with a different bare mass

$$m_{\mathbf{n}_d} = m + 2n_{d,1}r_1/a_1 + 2n_{d,2}r_2/a_2. \quad (2)$$

We note that the fermion doublers will interact with each other as soon as the four-Fermi coupling is switched on, playing a key role in the properties of the correlated Chern insulators.

Let us discuss the connection of Eq. (1) to SOC. In (2+1) dimensions, one can choose 2×2 gamma matrices, such that the spinor representation of rotations around the normal vector of the plane leads to field components $\psi_1(\mathbf{x}), \psi_2(\mathbf{x})$ that can be identified with spin up/down fermions. If one chooses $\gamma^0 = \sigma^z, \gamma^1 = i\sigma^x, \gamma^2 = -i\sigma^y$, the spin-flip tunnelings in Eq. (1), $\Psi^\dagger(\mathbf{x}) \frac{i\sigma^x}{2a_2} \Psi(\mathbf{x} + a_2 \mathbf{e}_2) - \Psi^\dagger(\mathbf{x}) \frac{i\sigma^y}{2a_1} \Psi(\mathbf{x} + a_1 \mathbf{e}_1)$, can be understood as the second-quantised lattice version of Rashba SOC $\mathbf{e}_3 \cdot (\mathbf{p} \wedge \boldsymbol{\sigma}) = i\sigma^x \partial_y - i\sigma^y \partial_x$ [9]. From this perspective, the combination of fermion bilinears (1) would correspond to a Dirac-type SOC [38] although, in view of the underlying discretisation [27], it might be more appropriate to refer to it as a *Dirac-Wilson SOC*. In contrast to (2+1) Gross-Neveu models [28], in which a discrete chiral symmetry $\Psi(\mathbf{x}) \rightarrow \gamma^5 \Psi(\mathbf{x})$ can be enforced using 4-component spinors, $\gamma^5 = i\gamma^0 \gamma^1 \gamma^2$ is simply the identity in our case, such that we can dispense with the notion of chiral symmetry. As discussed below, this has important consequences for the nature of the phases of Eq. (1).

Cold-atom quantum simulator.— We now describe a mapping of the couplings of the single-flavour Hamiltonian (1), where we choose the standard Dirac basis $\gamma^0 = \sigma^z, \gamma^1 = i\sigma^x, \gamma^2 = -i\sigma^y$, to the experimental parameters of ultra-cold atoms in *Raman optical lattices* [45–47]. To get a fully-tunable quantum simulator of Eq. (1) in this basis, we shall generalise the synthetic SOC scheme of [48, 49], such that atoms in

two states $\{|\uparrow\rangle, |\downarrow\rangle\}$ are subjected to the periodic potential

$$V = \frac{V_{0,1}}{2} \cos^2(kx_1) \mathbb{I}_2 + \frac{\tilde{V}_{0,1}}{2} \cos kx_1 e^{i(kx_2 - \Delta\omega t - \phi_1)} \boldsymbol{\sigma}^+ + \frac{V_{0,2}}{2} \cos^2(kx_2) \mathbb{I}_2 + \frac{\tilde{V}_{0,2}}{2} \cos kx_2 e^{i(kx_1 - \Delta\omega t - \phi_2)} \boldsymbol{\sigma}^+ + \text{H.c.} \quad (3)$$

Here, $V_{0,j}$ ($\tilde{V}_{0,j}$) stem from ac-Stark shifts (Rabi frequencies) of pairs of counter-propagating (orthogonal) laser beams with wavelength $\lambda = 2\pi/k$. The Raman term $\tilde{V}_{0,1}$ ($\tilde{V}_{0,2}$) with relative phase ϕ_1 (ϕ_2) induces a two-photon transition between the internal states $\boldsymbol{\sigma}^+ = |\uparrow\rangle\langle\downarrow|$ when the beatnote of the lasers is $\Delta\omega = \omega_0 - \delta$, where $\delta \ll \omega_0$ is the detuning. Accordingly, the atom absorbs a photon from the standing wave along x_1 (x_2), and emits it in the orthogonal travelling wave along x_2 (x_1). To minimise residual photon scattering and heating, one may consider lanthanide [50–52] or alkali-earth [53, 54] atoms.

As customary for ultra-cold atoms in optical lattices [55–57], in the regime of deep potentials $V_{0,j}, \tilde{V}_{0,j} \gg E_R = k^2/2m$, where m is the mass of the atoms, the dynamics of the gas can be expressed in terms of a lattice model where the atoms tunnel between neighbouring minima of the potential, and collide in pairs with an s -wave scattering length a_s . The specific interference pattern in Eq. (3) is crucial, as it ensures that the Raman terms do not contribute with on-site spin flips, but drive instead spin-flip tunnelings along the two spatial directions with a tunable relative phase. Using a basis of Wannier functions in the single-band approximation, and working in a rotating frame with respect to the Raman terms, one finds

$$H = - \sum_{\mathbf{n}, j} \left(t_j \left(f_{\mathbf{n}, \uparrow}^\dagger f_{\mathbf{n} + \mathbf{e}_j, \uparrow} + f_{\mathbf{n}, \downarrow}^\dagger f_{\mathbf{n} + \mathbf{e}_j, \downarrow} \right) + \text{H.c.} \right) - \sum_{\mathbf{n}, j} \left(i\tilde{t}_j e^{-i\phi_{j, \mathbf{n}}} \left(f_{\mathbf{n}, \uparrow}^\dagger f_{\mathbf{n} + \mathbf{e}_j, \downarrow} - f_{\mathbf{n}, \downarrow}^\dagger f_{\mathbf{n} - \mathbf{e}_j, \downarrow} \right) + \text{H.c.} \right) + \sum_{\mathbf{n}} U_{\uparrow\downarrow} f_{\mathbf{n}, \uparrow}^\dagger f_{\mathbf{n}, \downarrow}^\dagger f_{\mathbf{n}, \downarrow} f_{\mathbf{n}, \uparrow} + \frac{\delta}{2} \left(f_{\mathbf{n}, \uparrow}^\dagger f_{\mathbf{n}, \uparrow} - f_{\mathbf{n}, \downarrow}^\dagger f_{\mathbf{n}, \downarrow} \right), \quad (4)$$

where the fermionic operators $f_{\mathbf{n}, s}^\dagger$ ($f_{\mathbf{n}, s}$) create (annihilate) an atom in state $s \in \{\uparrow, \downarrow\}$ at a minimum of the ac-Stark shifts of Eq. (3), namely $\mathbf{x}_{\mathbf{n}}^0 = \sum_j \left(\frac{\lambda}{4} + \frac{\lambda}{2} n_j \right) \mathbf{e}_j$. Therefore, the terms above correspond to spin-independent tunnelings of strength $t_j = 4(E_R/\sqrt{\pi})(V_{0,j}/E_R)^{3/4} e^{-2\sqrt{V_{0,j}/E_R}}$, and contact Hubbard interactions of strength $U_{\uparrow\downarrow} = \sqrt{8/\pi} k_0 a_s E_R (V_{0,1} V_{0,2}/E_R^2)^{1/4}$. Using a Gaussian approximation for the Wannier functions, we obtain a spin-flip tunneling along the x_j -axis with strength $\tilde{t}_j = \tilde{V}_{0,j} e^{-(\pi^2/4)\sqrt{V_{0,j}/E_R}}$ and phase $\phi_{j, \mathbf{n}} = \phi_j - \pi(n_1 + n_2)$.

In order to find the mapping between the cold-atom model (4) and the four-Fermi lattice field theory (1) for $N = 1$, we must rescale the atomic operators such that they have the correct field units, and perform a gauge transformation $\Psi_{1,\uparrow}(\mathbf{x}_n^0) = f_{\mathbf{n},\uparrow}/\sqrt{a_1 a_2}$, $\Psi_{1,\downarrow}(\mathbf{x}_n^0) = e^{i\pi(n_1+n_2)} f_{\mathbf{n},\uparrow}/\sqrt{a_1 a_2}$. Setting the Raman-beam phases to $\phi_1 = 0, \phi_2 = \pi/2$, we find that model (4) maps directly to the lattice field theory (1) with

$$a_j = \frac{1}{2\tilde{t}_j}, \quad r_j = \frac{t_j}{\tilde{t}_j}, \quad m = \frac{\delta}{2} - 2(t_1 + t_2), \quad g^2 = \frac{U_{\uparrow\downarrow}}{4\tilde{t}_1\tilde{t}_2}. \quad (5)$$

Let us note the following important point. The expression above relates the anisotropic lattice spacings of the four-Fermi field theory (1) with the atom tunneling strengths, not with the distance $\lambda/2$ between neighbouring minima of the optical lattice. Therefore, taking the continuum limit in the lattice field theory (1) does not require sending the laser wavelength $\lambda \rightarrow 0$, but instead setting the experimental parameters ($t_j, \tilde{t}_j, \delta, U_{\uparrow\downarrow}$) to certain values, such that the bare couplings (m, a_j, r_j, g^2) lie in the vicinity of a critical point. Here, the energy gap is much smaller than the tunnelings $\Delta\epsilon \ll \tilde{t}_j$, and the relevant length scale $\xi \gg a_1, a_2$ leads to a continuum QFT.

Large- N quantum anomalous Hall effect.— In the non-interacting $g^2 = 0$ and isotropic $a_1 = a_2 =: a, r_1 = r_2 = 1$ limits, the single-flavour Hamiltonian (1) corresponds to the square-lattice version [20, 21] of Haldane’s model [19, 58] of the quantum anomalous Hall (QAH) effect [25]. This QAH effect has been realised in semiconducting ferromagnetic films [59, 60], observing a quantised conductance transverse to a bias potential for vanishing magnetic fields. Regarding Eq. (1), this quantisation depends on the Chern number via

$$\sigma_{xy} = \frac{e^2}{h} N_{\text{Ch}}, \quad N_{\text{Ch}} = \frac{N}{2} \sum_{\mathbf{n}_d} (-1)^{(n_{d,1} + n_{d,2})} \text{sign}(m_{\mathbf{n}_d}). \quad (6)$$

According to the doubler masses (2), and using Eq. (6) in the single-flavour limit $N = 1$, one finds that the Chern number is quantised to a non-zero integer $N_{\text{Ch}} = -1$ when $ma \in (-2, 0)$, whereas $N_{\text{Ch}} = +1$ when $ma \in (-4, -2)$, both of which lead to a QAH phase, i.e. a Chern insulator, and $N_{\text{Ch}} = 0$ otherwise. Let us note, however, that the spinor components correspond to bonding/anti-bonding orbitals of the upper/lower surface states of these semiconducting thin films [59, 60]. Correlation effects, which do not seem to play any role in these thin films [59, 60] would not be described, in any case, by the Lorentz-invariant four-Fermi term (1). Instead, for cold atoms with the Dirac Wilson SOC (4), the spinor is formed by two internal states that interact naturally via such a four-Fermi term. The key advantage of the cold-atom realisation hereby proposed is that the coupling strength g^2 , as well as all other microscopic parameters (5), can be experimentally tuned. This brings a unique opportunity to realise correlated Chern insulators with a neat connection to strongly-coupled QFTs originally considered in high-energy physics. In this context [61–67], topological insulators in different symmetry classes and dimensions [68] correspond to lower-dimensional versions of the so-called domain-wall fermions [69], where

the topological invariants control a Chern-Simons-type response to external gauge fields [21, 70–72].

Let us now describe the fate of these Chern insulators and the QAH effect as we switch on interactions $g^2 > 0$. From the analogy with the Gross-Neveu (GN) model [33], one expects that the phenomenon of dynamical mass generation by the formation of a homogeneous scalar condensate $\Sigma_0 \propto \langle \bar{\Psi}(\mathbf{x})\Psi(\mathbf{x}) \rangle$ will play an important role. We note, however, that due to the particular representation of the gamma matrices, this condensate will not be associated to chiral symmetry breaking as would occur for the (1+1) version [33, 63–67], or for (2+1) models with a non-trivial γ^5 matrix [28, 29]. If such models are discretised following the Wilson prescription, the fermions can also form a pseudo-scalar condensate $\Pi_0 \propto \langle \bar{\Psi}(\mathbf{x})i\gamma^5\Psi(\mathbf{x}) \rangle$ through the spontaneous breakdown of parity $\Psi(\mathbf{x}) \rightarrow \gamma^0\Psi(-\mathbf{x})$ [73, 74]. In contrast, we identify two different π -condensates $\Pi_1 \propto \langle \bar{\Psi}(\mathbf{x})\gamma^1\Psi(\mathbf{x}) \rangle$ and $\Pi_2 \propto \langle \bar{\Psi}(\mathbf{x})\gamma^2\Psi(\mathbf{x}) \rangle$, the non-zero values of which also lead to the spontaneous breakdown of the discrete parity symmetry and, additionally, to the breakdown of Lorentz-invariance even in the long-wavelength limit. In the language of the underlying Hubbard model with SOC (4), these π -condensates correspond to two orthogonal ferromagnetic orders, namely $\Pi_1 \propto \langle f_{\mathbf{n},\uparrow}^\dagger f_{\mathbf{n},\downarrow} \rangle + \langle f_{\mathbf{n},\downarrow}^\dagger f_{\mathbf{n},\uparrow} \rangle$, and $\Pi_2 \propto i\langle f_{\mathbf{n},\uparrow}^\dagger f_{\mathbf{n},\downarrow} \rangle - i\langle f_{\mathbf{n},\downarrow}^\dagger f_{\mathbf{n},\uparrow} \rangle$, which break the combined \mathbb{Z}_2 spin and lattice inversions.

In order to understand how these condensates affect the Chern insulator and QAH phases discussed above, we make use of non-perturbative *large- N techniques* developed in the context of QFTs in Euclidean spacetime $x = (it, \mathbf{x})$ [75]. Let us outline our calculation. First of all, we introduce three auxiliary scalar fields $\sigma(x), \pi_1(x), \pi_2(x)$, which do not propagate, but act instead as mediators of the contact four-Fermi term (1). This allows us to organise the Feynman diagrams of the QFT according to their order in N , and identify the leading contribution when $N \rightarrow \infty$, which contains diagrams with a single fermion loop and an even number of external lines for the auxiliary fields. In this way, we can obtain analytically the radiative corrections to the classical potential, which contain the leading-order contribution [33, 76] to the *effective potential* [77]. In our case, we are interested in the effective potential for $\boldsymbol{\pi}(x) = (\pi_1(x), \pi_2(x))$, the minimum of which can be used to locate the spontaneous breakdown of parity $\boldsymbol{\Pi} := (\Pi_1, \Pi_2) = \langle \boldsymbol{\pi}(x) \rangle \neq \mathbf{0}, \forall x$. By resumming the diagrams to all orders of the coupling strength, we obtain

$$\begin{aligned} \frac{V_{\text{eff}}(\tilde{\boldsymbol{\Pi}})}{N} &= \frac{\tilde{\boldsymbol{\Pi}}^2}{2\tilde{g}^2} - \sum_k \log \left(1 + \frac{\sum_\mu \tilde{\Pi}_\mu^2}{M_k^2 + \sum_\mu p_{\mu,k}^2} \right) \\ &\quad - \frac{1}{2} \sum_k \log \left(1 - \left(\frac{2\sum_\mu \tilde{\Pi}_\mu p_{\mu,k}}{M_k^2 + \sum_\mu (p_{\mu,k}^2 + \tilde{\Pi}_\mu^2)} \right)^2 \right), \end{aligned} \quad (7)$$

where we work in discretised Euclidean time with spacing a_0 and anti-periodic boundary conditions after N_0 time steps, such that the momentum lies in the Brillouin zone $k = (k_0, \mathbf{k}) \in \text{BZ} = [-\pi, \pi]^3$. Here, we have introduced the short-hand notation $\sum_k = \sum_{k \in \text{BZ}} / N_0 N_1 N_2$, $p_{\mu,k} = 2\kappa_\mu \sin k_\mu$, and $M_k = \tilde{m} + 1 - 2\kappa_\mu \cos k_\mu + \tilde{\Sigma}_0$, with $\kappa_\mu = 1/2a_\mu (\sum_\nu a_\nu^{-1})$,

and $r_\mu = 1$. As customary in lattice field theory, we work with dimensionless quantities [78], and we set $\tilde{\Gamma}_0 = 0$ above.

We now minimise the effective potential considering a homogeneous scalar condensate $\Sigma_0 = \langle \sigma(x) \rangle \forall x$, and then obtain its value by evaluating self-consistently the corresponding tad-pole diagram at the minimum of the effective potential

$$\tilde{\Sigma}_0 = \tilde{g}^2 \sum_k \frac{M_k}{M_k^2 + \sum_\mu (p_{\mu,k} + \tilde{\Pi}_\mu)^2}. \quad (8)$$

From this pair of equations (7)-(8), one can extract all effects of correlations on the large- N QAH effect. First of all, in the parity-symmetric phases where none of the π fields condense, we find a non-zero scalar condensate $\Sigma_0(g^2) \neq 0$ for any $g^2 > 0$ [79]. This condensate contributes to the static part of the fermionic self-energy $\Sigma(0, \mathbf{k}) = \Sigma_0(g^2) \gamma^0$ defined via the inverse of the interacting Green's function $G^{-1}(ik_0, \mathbf{k}) = ik_0 - (M_k \gamma^0 + \sum_j p_{j,k} \gamma^j) + \Sigma(ik_0, \mathbf{k})$, which is obtained from the Fourier and Matsubara transforms of the Euclidean two-point function $G(x-y) = \langle \mathcal{S} \{ \Psi^\dagger(x) \Psi(y) \} \rangle$. Remarkably, the static self-energy can be used for a practical calculation [82–84] of topological invariants [85] beyond the non-interacting limit [86]. In our case, we obtain a closed expression for the dependence of the Chern number on the interaction strength

$$N_{\text{Ch}}(g^2) = \frac{N}{2} \sum_{n_d} (-1)^{(n_{d,1} + n_{d,2})} \text{sign}(m_{n_d} + \Sigma_0(g^2)), \quad (9)$$

which can be used to predict the existence of correlated QAH phases in which the interacting fermions still display a quantised transverse conductivity $\sigma_{xy} = \pm \frac{e^2}{h} N$. These regions, depicted in Fig. 1, show that the correlated Chern insulators are very robust, surviving for considerably large interactions with respect to the free-fermion QAH phase (6).

Let us now discuss the π condensation, which occurs via two possible channels depending on the anisotropy, $(\Pi_1, 0)$ for $a_1 > a_2$, or $(0, \Pi_2)$ for $a_1 < a_2$, each of which corresponds to ferromagnetic ordering along a different axis [87]. As clarified below, this ordering differs from the standard ferromagnetism found in solid-state materials as, in particular, the low-energy excitations in this ferromagnet will be gapped. The set of parameters where the π condensates form define critical lines that separate the correlated QAH phase from a long-range-ordered ferromagnet (FM), as depicted in Fig. 1. From a closer analysis of the effective potential, we note that these critical lines describe second-order quantum phase transitions which, interestingly, become first-order around the central region. This will be discussed in detail in future work [88].

Quantum compass model and projected-entangled pairs.– The above results have unveiled a rich phase diagram with correlated Chern insulators, trivial band insulators, and ferromagnetic parity-broken phases, separated by critical lines related to the specific values of σ and π condensates, and controlled by strongly-coupled QFTs. However, these predictions are strictly valid in the $N \rightarrow \infty$ limit, whereas the cold-atom realisation of SOC (4) yields $N = 1$. Although future experiments could validate if our large- N predictions survive in the ultimate quantum limit of $N = 1$, exploring the characteristic

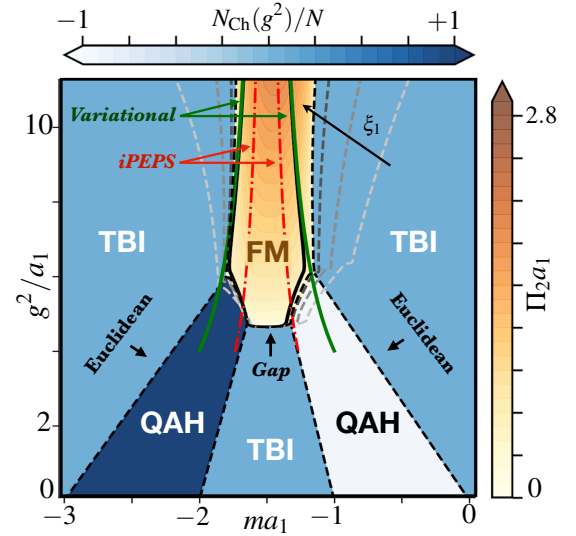


Figure 1. **Phase diagram of the four-Fermi QFT:** Contour plots of the Chern number N_{Ch} (blue) and π condensate (orange) for $a_2 = 2a_1$, predicting a large- N quantum anomalous Hall (QAH) effect, trivial band insulators (TBIs), and a ferromagnetic phase (FM). These phases are separated by dashed lines (Euclidean) obtained from Eqs. (7)-(8) in grey scale with an increasing time-like anisotropy $\xi_1 = a_1/a_0 \in \{10, 20, 40, 64\}$. The black solid line is obtained by solving self-consistent equations (Gap) in the time-continuum limit $a_0 \rightarrow 0$, which can only delimit the area of the FM, but give no further information about the TBI or QAH phases. The green solid lines represent the product-state prediction for the compass model (Variational) in Eq. (12), whereas the red dashed-dotted lines incorporate quantum correlations by the use of iPEPs.

scaling of the strongly-coupled fixed points, it would be reassuring to have a partial confirmation with different methods.

Exploiting the connection of the four-Fermi lattice theory (1) to the Hubbard model with SOC (4), we can derive an effective description for the strong-coupling limit $g^2 \gg 1$ using the concept of magnetic exchange interactions [89, 90]. This limit is governed by second-order processes, by which the fermions tunnel back and forth forming virtual double occupancies. In contrast to the standard Hubbard model, where this leads to Heisenberg interactions [91], we obtain

$$H_{\text{eff}} = \sum_{\mathbf{x} \in \Lambda_s} (J_x \tau_{\mathbf{x}}^x \tau_{\mathbf{x}+a_2 \mathbf{e}_2}^x + J_y \tau_{\mathbf{x}}^y \tau_{\mathbf{x}+a_1 \mathbf{e}_1}^y - h \tau_{\mathbf{x}}^z). \quad (10)$$

Here, the bi-linears $\{\tau_{\mathbf{x}}^\alpha = a_1 a_2 \Psi^\dagger(\mathbf{x}) \sigma^\alpha \Psi(\mathbf{x})\}_{\alpha=x,y,z}$ yield the spin-1/2 operators $\mathcal{S}_{\mathbf{x}} = \frac{1}{2} \tau_{\mathbf{x}}$ of the SOC model, and

$$J_x = -\frac{a_1}{2a_2 g^2} = -\frac{2\tilde{t}_2^2}{U_{\uparrow\downarrow}}, \quad J_y = -\frac{a_2}{2a_1 g^2} = -\frac{2\tilde{t}_1^2}{U_{\uparrow\downarrow}}, \quad (11)$$

are the exchange couplings, while $h = (m + a_1^{-1} + a_2^{-2})$ is a transverse field. This spin model belongs to the family of *quantum compass models* [92], which have a characteristic directionality of the spin-spin interactions that is responsible for the appearance of topologically-ordered phases of matter with anionic excitations in the honeycomb lattice [93]. For our

rectangular lattice, the anisotropic compass model has been thoroughly studied for a vanishing transverse field $h = 0$ [92]. In this case, there are gauge-like symmetries [94] that enforce a 2-fold degeneracy of the eigenstates, and can be exploited to encode a logical qubit for fault-tolerant quantum computing [95, 96]. As one tunes the exchange couplings across the symmetric point $J_x = J_y$, a first-order phase transition between two gapped ferromagnetic orders has been detected [97–99], i.e. $\langle \tau_x^x \rangle \neq 0$ when $J_x > J_y$, and $\langle \tau_x^y \rangle \neq 0$ when $J_x < J_y$.

In contrast to the zero-field case, to the best of our knowledge, the transverse-field quantum compass model remains largely unexplored. Note that the above order parameters correspond exactly to the previously introduced π condensates which, according to our large- N results, may also appear for $h \neq 0$. We have performed a variational study of the model using two different *Ansätze*. On the one hand, a simple separable state where all spins point in a given direction along the equatorial plane allows us to predict two types of second-order phase transitions with the following orderings

$$\begin{aligned} \langle \tau_x^x \rangle &= \Pi_1 = \left(1 - \frac{h^2}{4J_x^2}\right)^{1/2}, & \text{if } 2|J_x| \geq |h|, J_y > J_x, \\ \langle \tau_x^y \rangle &= \Pi_2 = \left(1 - \frac{h^2}{4J_y^2}\right)^{1/2}, & \text{if } 2|J_y| \geq |h|, J_y < J_x, \end{aligned} \quad (12)$$

The groundstate displays a $\Pi_1 \propto \langle \tau_x^x \rangle$ ($\Pi_2 \propto \langle \tau_x^y \rangle$) condensate for $J_x < J_y < 0$ ($J_y < J_x < 0$) which, according to Eq. (11), occurs for $a_1 > a_2$ ($a_1 < a_2$) in agreement with the large- N results. These critical lines are compared to the large- N prediction in Fig. 1, showing a remarkable agreement for sufficiently strong couplings. Finally, we have also used an infinite projected-entangled-pairs (iPEPS) ansatz [100–102] for the groundstate of Eq. (10). The iPEPS is a powerful framework for the simulation of 2D strongly-correlated models, which captures the interplay of locality and entanglement by expressing an entangled many-body wave-function in terms of local tensors. We have implemented the variational iPEPS algorithms described in [103–105], the accuracy of which relies

on a refinement parameter D related to the maximum entanglement content of the ansatz. In practice, increasing D leads to better descriptions of the ground state, and $D = 2$ is the minimum value that captures the effect of quantum correlations. In Fig. 1 (red line), we present the results for $D = 2$ obtained by locating the divergence of the magnetic susceptibility $\chi_j = \partial M_j / \partial h$. As shown in [99] for the $h = 0$ model (10), iPEPS with $D = 2$ already yields better results than those obtained by combining fermionization with mean-field theory. We have checked that, for $h \neq 0$, iPEPS also provides significantly-lower variational energies than the ones obtained by large- N or the separable-state mean-field ansatz, which typically under-estimate the effect of the transverse field. This has allowed us to draw a more accurate prediction with a clear displacement of the critical lines and a narrower FM region.

Outlook.– We have shown that 2D Hubbard models with Dirac-Wilson SOC, which can be realised with neutral atoms in Raman lattices, give access to the ultimate quantum limit of strongly-coupled QFTs hosting correlated Chern insulators and displaying a QAH effect. The framework hereby presented can serve as the stepping stone to address open questions, such as finite fermion densities in search for a cold-atom realisations of fractional QAH effects [106, 107] and contemporary relativistic QFTs with fractionalisation [108].

Acknowledgements.– We are very grateful to Luca Tagliacozzo for fruitful discussions. This project has received funding from the European Union’s Horizon 2020 research and innovation programme under the Marie Skłodowska-Curie grant agreement No 665884, the Spanish Ministry MINECO (National Plan 15 Grant: FISICATEAMO No. FIS2016-79508-P, SEVERO OCHOA No. SEV-2015-0522, FPI), European Social Fund, Fundació Cellex, Generalitat de Catalunya (AGAUR Grant No. 2017 SGR 1341, CERCA/Program), ERC AdG NOQIA, EU FEDER, and the National Science Centre, Poland-Symfonia Grant No. 2016/20/W/ST4/00314. The work of S.J.H. was supported by STFC grant ST/L000369/1. A.B. acknowledges support from the Ramón y Cajal program RYC-2016-20066, CAM/FEDER Project S2018/TCS- 4342 (QUITEMADCM), and PGC2018-099169-B-I00 (MCIU/AEI/FEDER, UE).

-
- [1] L. H. Thomas, *Nature* **117**, 514 (1926).
 - [2] P. A. M. Dirac, *Proceedings of the Royal Society of London. Series A* **117**, 610 (1928).
 - [3] P. A. M. Dirac, *Proceedings of the Royal Society of London. Series A* **126**, 360 (1930).
 - [4] S. S. Schweber, *QED and the Men Who Made It: Dyson, Feynman, Schwinger, and Tomonaga*, Vol. 104 (Princeton University Press, 1994).
 - [5] J. Schwinger, *Phys. Rev.* **73**, 416 (1948).
 - [6] T. Aoyama, M. Hayakawa, T. Kinoshita, and M. Nio, *Phys. Rev. Lett.* **109**, 111807 (2012).
 - [7] D. Hanneke, S. Fogwell, and G. Gabrielse, *Phys. Rev. Lett.* **100**, 120801 (2008).
 - [8] R. H. Parker, C. Yu, W. Zhong, B. Estey, and H. Müller, *Science* **360**, 191 (2018).
 - [9] Y. A. Bychkov and E. I. Rashba, *Journal of Physics C: Solid State Physics* **17**, 6039 (1984).
 - [10] G. Dresselhaus, *Phys. Rev.* **100**, 580 (1955).
 - [11] M. König, S. Wiedmann, C. Brüne, A. Roth, H. Buhmann, L. W. Molenkamp, X.-L. Qi, and S.-C. Zhang, *Science* **318**, 766 (2007).
 - [12] D. Hsieh, D. Qian, L. Wray, Y. Xia, Y. S. Hor, R. J. Cava, and M. Z. Hasan, *Nature* **452**, 970 EP (2008).
 - [13] C. L. Kane and E. J. Mele, *Phys. Rev. Lett.* **95**, 146802 (2005).
 - [14] C. L. Kane and E. J. Mele, *Phys. Rev. Lett.* **95**, 226801 (2005).
 - [15] B. A. Bernevig, T. L. Hughes, and S.-C. Zhang, *Science* **314**, 1757 (2006).
 - [16] M. Z. Hasan and C. L. Kane, *Rev. Mod. Phys.* **82**, 3045 (2010).
 - [17] X.-L. Qi and S.-C. Zhang, *Rev. Mod. Phys.* **83**, 1057 (2011).
 - [18] C.-K. Chiu, J. C. Y. Teo, A. P. Schnyder, and S. Ryu, *Rev. Mod. Phys.* **88**, 035005 (2016).
 - [19] F. D. M. Haldane, *Phys. Rev. Lett.* **61**, 2015 (1988).

- [20] X.-L. Qi, Y.-S. Wu, and S.-C. Zhang, *Phys. Rev. B* **74**, 085308 (2006).
- [21] X.-L. Qi, T. L. Hughes, and S.-C. Zhang, *Phys. Rev. B* **78**, 195424 (2008).
- [22] M. Nakahara, *Geometry, Topology and Physics* (CRC Press, 2017).
- [23] S.-S. Chern, *Annals of Mathematics* **47**, 85 (1946).
- [24] F. D. M. Haldane, *Rev. Mod. Phys.* **89**, 040502 (2017).
- [25] C.-X. Liu, S.-C. Zhang, and X.-L. Qi, *Annual Review of Condensed Matter Physics* **7**, 301 (2016).
- [26] A. Soumyanarayanan, N. Reyren, A. Fert, and C. Panagopoulos, *Nature* **539**, 509 (2016).
- [27] K. G. Wilson, in *New Phenomena in Subnuclear Physics* (Springer US, 1977) pp. 69–142.
- [28] S. Hands, A. Kocic, and J. Kogut, *Annals of Physics* **224**, 29 (1993).
- [29] S. Hands, “Fixed point four-fermi theories,” (1997), [arXiv:hep-lat/9706018](https://arxiv.org/abs/hep-lat/9706018).
- [30] J. Braun, *Journal of Physics G: Nuclear and Particle Physics* **39**, 033001 (2012).
- [31] E. Fermi, *Zeitschrift für Physik* **88**, 161 (1934).
- [32] Y. Nambu and G. Jona-Lasinio, *Phys. Rev.* **122**, 345 (1961).
- [33] D. J. Gross and A. Neveu, *Phys. Rev. D* **10**, 3235 (1974).
- [34] J. Hubbard, *Proc. R. Soc. London, Ser. A* **276**, 238 (1963).
- [35] K. G. Wilson, *Phys. Rev. D* **10**, 2445 (1974).
- [36] C. Gattringer and C. B. Lang, *Quantum chromodynamics on the lattice: an introductory presentation* (Springer, 2010).
- [37] V. Galitski and I. B. Spielman, *Nature* **494**, 49 (2013).
- [38] L. Zhang and X.-J. Liu, “Spin-orbit coupling and topological phases for ultracold atoms,” in *Synthetic Spin-Orbit Coupling in Cold Atoms*, Chap. Chapter 1, pp. 1–87.
- [39] R. P. Feynman, *Int. J. Theor. Phys.* **21**, 467 (1982).
- [40] M. Lewenstein, A. Sanpera, V. Ahufinger, B. Damski, A. Sen(De), and U. Sen, *Advances in Physics* **56**, 243 (2007).
- [41] I. Bloch, J. Dalibard, and S. Nascimbène, *Nature Physics* **8**, 267 (2012).
- [42] J. Kogut and L. Susskind, *Phys. Rev. D* **11**, 395 (1975).
- [43] H. Nielsen and M. Ninomiya, *Nuclear Physics B* **185**, 20 (1981).
- [44] H. Nielsen and M. Ninomiya, *Nuclear Physics B* **193**, 173 (1981).
- [45] Z. Wu, L. Zhang, W. Sun, X.-T. Xu, B.-Z. Wang, S.-C. Ji, Y. Deng, S. Chen, X.-J. Liu, and J.-W. Pan, *Science* **354**, 83 (2016), NoStop
- [46] W. Sun, B.-Z. Wang, X.-T. Xu, C.-R. Yi, L. Zhang, Z. Wu, Y. Deng, X.-J. Liu, S. Chen, and J.-W. Pan, *Phys. Rev. Lett.* **121**, 150401 (2018).
- [47] B. Song, L. Zhang, C. He, T. F. J. Poon, E. Hajiyeve, S. Zhang, X.-J. Liu, and G.-B. Jo, *Science Advances* **4** (2018).
- [48] X.-J. Liu, K. T. Law, and T. K. Ng, *Phys. Rev. Lett.* **112**, 086401 (2014).
- [49] X.-J. Liu, K. T. Law, and T. K. Ng, *Phys. Rev. Lett.* **113**, 059901 (2014).
- [50] N. Q. Burdick, Y. Tang, and B. L. Lev, *Phys. Rev. X* **6**, 031022 (2016).
- [51] B. Song, C. He, S. Zhang, E. Hajiyeve, W. Huang, X.-J. Liu, G.-B. Jo, *Phys. Rev. A* **94**, 061604 (2016).
- [52] L. F. Livi, G. Cappellini, M. Diem, L. Franchi, C. Clivati, M. Frittelli, F. Levi, D. Calonico, J. Catani, M. Inguscio, and L. Fallani, *Phys. Rev. Lett.* **117**, 220401 (2016).
- [53] S. Kolkowitz, S. L. Bromley, T. Bothwell, M. L. Wall, G. E. Marti, A. P. Koller, X. Zhang, A. M. Rey, and J. Ye, *Nature* **542**, 66 (2017).
- [54] S. L. Bromley, S. Kolkowitz, T. Bothwell, D. Kedar, A. Safavi-Naini, M. L. Wall, C. Salomon, A. M. Rey, and J. Ye, *Nature Phys.* **14**, 399 (2018).
- [55] D. Jaksch, C. Bruder, J. I. Cirac, C. W. Gardiner, and P. Zoller, *Phys. Rev. Lett.* **81**, 3108 (1998).
- [56] W. Hofstetter, J. I. Cirac, P. Zoller, E. Demler, and M. D. Lukin, *Phys. Rev. Lett.* **89**, 220407 (2002).
- [57] I. Bloch, J. Dalibard, and W. Zwerger, *Rev. Mod. Phys.* **80**, 885 (2008).
- [58] G. Jotzu, M. Messer, R. Desbuquois, M. Lebrat, T. Uehlinger, D. Greif, and T. Esslinger, *Nature* **515**, 237 (2014).
- [59] C.-Z. Chang, J. Zhang, X. Feng, J. Shen, Z. Zhang, M. Guo, K. Li, Y. Ou, P. Wei, L.-L. Wang, Z.-Q. Ji, Y. Feng, S. Ji, X. Chen, J. Jia, X. Dai, Z. Fang, S.-C. Zhang, K. He, Y. Wang, L. Lu, X.-C. Ma, and Q.-K. Xue, *Science* **340**, 167 (2013).
- [60] C.-Z. Chang, W. Zhao, D. Y. Kim, H. Zhang, B. A. Assaf, D. Heiman, S.-C. Zhang, C. Liu, M. H. W. Chan, and J. S. Moodera, *Nature Materials* **14**, 473 (2015).
- [61] A. Bermudez, L. Mazza, M. Rizzi, N. Goldman, M. Lewenstein, and M. A. Martin-Delgado, *Phys. Rev. Lett.* **105**, 190404 (2010).
- [62] D. B. Kaplan and S. Sun, *Phys. Rev. Lett.* **108**, 181807 (2012).
- [63] J. Jünemann, A. Piga, S.-J. Ran, M. Lewenstein, M. Rizzi, and A. Bermudez, *Phys. Rev. X* **7**, 031057 (2017).
- [64] A. Bermudez, E. Tirrito, M. Rizzi, M. Lewenstein, and S. Hands, *Annals of Physics* **399**, 149 (2018).
- [65] Y. Kuno, *Phys. Rev. B* **99**, 064105 (2019).
- [66] E. Tirrito, M. Rizzi, G. Sierra, M. Lewenstein, and A. Bermudez, *Phys. Rev. B* **99**, 125106 (2019).
- [67] G. Roose, N. Bultinck, L. Vanderstraeten, F. Verstraete, K. Van Acoleyen, and J. Haegeman, [arXiv:2010.03441](https://arxiv.org/abs/2010.03441) (2020).
- [68] S. Ryu, A. P. Schnyder, A. Furusaki, and A. W. W. Ludwig, *New Journal of Physics* **12**, 065010 (2010).
- [69] D. B. Kaplan, *Physics Letters B* **288**, 342 (1992).
- [70] H. So, *Progress of Theoretical Physics* **73**, 528 (1985).
- [71] M. F. Golterman, K. Jansen, and D. B. Kaplan, *Physics Letters B* **301**, 219 (1993).
- [72] S. Sen, “Chern insulator transitions with wilson fermions on a hyperrectangular lattice,” (2020), [arXiv:2008.01743](https://arxiv.org/abs/2008.01743).
- [73] S. Aoki, *Phys. Rev. D* **30**, 2653 (1984).
- [74] S. Sharpe and R. Singleton, *Phys. Rev. D* **58**, 074501 (1998).
- [75] S. Coleman, *Aspects of Symmetry: Selected Erice Lectures* (Cambridge University Press, 1985).
- [76] S. Coleman, R. Jackiw, and H. D. Politzer, *Phys. Rev. D* **10**, 2491 (1974).
- [77] S. Coleman and E. Weinberg, *Phys. Rev. D* **7**, 1888 (1973).
- [78] In Euclidean anisotropic lattices, dimensionless fields have a symmetric rescaling $\Psi(\mathbf{x}) = \tilde{\Psi}(\mathbf{x})/\sqrt{a_0 a_1 + a_1 a_2 + a_2 a_0}$. This leads to the following dimensionless bare mass $\tilde{m} = ma_1/(1 + \xi_1 + \xi_2)$ with $\xi_1 = a_1/a_0$ and $\xi_2 = a_1/a_2$, and coupling strength $\tilde{g}^2 = (g^2/a_1)\xi_1\xi_2/(1 + \xi_1 + \xi_2)^2$. Additionally, due to the presence of additional doublers in the time direction, there is an additive renormalisation $\tilde{m} \rightarrow \tilde{m} - \frac{1}{2}\tilde{g}^2(1 + \xi_1 + \xi_2)^2/\xi_1$. The condensates become dimensionless through $\tilde{\Sigma}_0 = \Sigma_0 a_1/(1 + \xi_1 + \xi_2)$, and $\tilde{\Pi} = \Pi a_1/(1 + \xi_1 + \xi_2)$.
- [79] Only in the isotropic case, $a_1 = a_2 =: a$, and along the symmetric line $(-ma, g^2) = (2, g^2)$, does the scalar condensate vanish for any coupling strength $\Sigma_0(g^2) = 0$, which signals a cancellation of the additive mass renormalisations arising from the two fermion doublers at $\mathbf{k} \in \{(0, \pi/a), (\pi/a, 0)\}$. The lack of additive renormalisation in this so-called *central Wilson branch* is not a large- N artefact, which has interesting implications for Monte Carlo studies of other lattice gauge theories [80, 81].

- [80] T. Misumi and Y. Tanizaki, *Progress of Theoretical and Experimental Physics* **2020** (2020), 10.1093/ptep/ptaa003, 033B03.
- [81] T. Misumi and J. Yumoto, “Varieties and properties of central-branch wilson fermions,” (2020), [arXiv:2005.08857](https://arxiv.org/abs/2005.08857).
- [82] Z. Wang and S.-C. Zhang, *Phys. Rev. X* **2**, 031008 (2012).
- [83] Z. Wang and S.-C. Zhang, *Phys. Rev. B* **86**, 165116 (2012).
- [84] Z. Wang and B. Yan, *Journal of Physics: Condensed Matter* **25**, 155601 (2013).
- [85] Z. Wang, X.-L. Qi, and S.-C. Zhang, *Phys. Rev. Lett.* **105**, 256803 (2010).
- [86] D. J. Thouless, M. Kohmoto, M. P. Nightingale, and M. den Nijs, *Phys. Rev. Lett.* **49**, 405 (1982).
- [87] At the isotropic point $a_1 = a_2 =: a$, there is an additional $O(2)$ symmetry, such that the parity-broken phase will spontaneously select the direction of the ferromagnetic order in the xy -plane. In this limit, one can also envisage the appearance of a Chern-Simons term which, by its very nature, can only influence dynamics while our large- N solution focusses on static properties. The consequences of this term will be studied in the future [88].
- [88] L. Ziegler et al., (in preparation) (2020).
- [89] P. W. Anderson, *Phys. Rev.* **79**, 350 (1950).
- [90] P. W. Anderson (Academic Press, 1963) pp. 99 – 214.
- [91] W. Heisenberg, *Zeitschrift für Physik* **49**, 619 (1928).
- [92] Z. Nussinov and J. van den Brink, *Rev. Mod. Phys.* **87**, 1 (2015).
- [93] A. Kitaev, *Annals of Physics* **321**, 2 (2006),.
- [94] B. Douçot, M. V. Feigel’man, L. B. Ioffe, and A. S. Ioselevich, *Phys. Rev. B* **71**, 024505 (2005).
- [95] D. Bacon, *Phys. Rev. A* **73**, 012340 (2006).
- [96] M. Li, D. Miller, M. Newman, Y. Wu, and K. R. Brown, *Phys. Rev. X* **9**, 021041 (2019).
- [97] J. Dorier, F. Becca, and F. Mila, *Phys. Rev. B* **72**, 024448 (2005).
- [98] H.-D. Chen, C. Fang, J. Hu, and H. Yao, *Phys. Rev. B* **75**, 144401 (2007).
- [99] R. Orús, A. C. Doherty, and G. Vidal, *Phys. Rev. Lett.* **102**, 077203 (2009).
- [100] F. Verstraete and J. I. Cirac, [arXiv:cond-mat/0407066](https://arxiv.org/abs/cond-mat/0407066) (2004).
- [101] J. Jordan, R. Orús, G. Vidal, F. Verstraete, and J.I Cirac, *Phys. Rev. Lett.* **101**, 250602 (2008).
- [102] H. C. Jiang, Z. Y. Weng, and T. Xiang, *Phys. Rev. Lett.* **101**, 090603 (2008).
- [103] R. Orús, and G. Vidal, *Phys. Rev. B* **80**, 094403 (2009).
- [104] H. N. Phien, J. A. Bengua, H. D. Tuan, P. Corboz, and R. Orús, *Phys. Rev. B* **92**, 035142 (2015).
- [105] P. Corboz, *Phys. Rev. B* **94**, 035133 (2016).
- [106] D.N. Sheng, Z.-C. Gu, K. Sun, and L. Sheng, *Nature Comm.* **2**, 389 (2011).
- [107] T. Neupert, L. Santos, C. Chamon, and C. Mudry, *Phys. Rev. Lett.* **106**, 236804 (2011).
- [108] D. B. Kaplan and S. Sen, *Phys. Rev. Lett.* **124**, 131601 (2020).